LOCAL SEGMENTATION BY LARGE SCALE HYPOTHESIS TESTING
Segmentation as Outlier Detection

Sune Darkner, Anders B. Dahl, Rasmus Larsen
DTU Informatics, Technical University of Denmark, Richard Petersens plads, Kgs. Lyngby, Denmark

Arnold Skimminge, Ellen Garde, Gunhild Waldemar
DRCMR, Copenhagen University Hospital Hvidovre, Kettegaard Alle 30, DK 2650 Hvidovre, Denmark
Memory Disorders Research Group, Department of Neurology, Copenhagen University Hospital, Copenhagen, Denmark

Keywords: Segmentation, Outlier detection, Large scale hypothesis testing, Locally adjusted threshold.

Abstract: We propose a novel and efficient way of performing local image segmentation. For many applications a threshold of pixel intensities is sufficient. However, determining the appropriate threshold value poses a challenge. In cases with large global intensity variation the threshold value has to be adapted locally. We propose a method based on large scale hypothesis testing with a consistent method for selecting an appropriate threshold for the given data. By estimating the prominent distribution we characterize the segment of interest as a set of outliers or the distribution it self. Thus, we can calculate a probability based on the estimated densities of outliers actually being outliers using the false discovery rate (FDR). Because the method relies on local information it is very robust to changes in lighting conditions and shadowing effects. The method is applied to endoscopic images of small particles submerged in fluid captured through a microscope and we show how the method can handle transparent particles with significant glare point. The method generalizes to other problems. This is illustrated by applying the method to camera calibration images and MRI of the midsagittal plane for gray and white matter separation and segmentation of the corpus callosum. Comparing this segmentation method with manual corpus callosum segmentation an average dice score of 0.88 is obtained across 40 images.

1 INTRODUCTION

We present a novel way of performing binary segmentation of images with large global variations. In many segmentation problems such as global changes in illumination, shadows, or background variations, a global threshold is not a feasible solution. Variations in pixel intensities can result in large segmentation errors if one global threshold value is applied. As a consequence the threshold has to be locally adapted. Another problem is the dominating background intensities, which makes typical histogram based methods like histogram clustering (Otsu, 1975) inappropriate.

We propose a method based on the assumption that a local threshold exists, which will separate the segment of interest from the background. We present a well defined way of selecting the appropriate threshold value given the observations based on a large scale hypothesis test and experimentally show that this assumption is appropriate for many real segmentation problems.

2 PREVIOUS WORK

Segmentation is a widely used technique in computer vision for identifying regions of interest. Basic threshold is a simple, very robust and fast approach for performing segmentation. It is applicable for a wide range of segmentation problems where regions of interest have intensity levels which differers from the remainder of the scene. Many techniques have been developed for identification of suitable threshold.(Sezgin and Sankur, 2004) gives an overview. The simplest approach is to perform a global threshold for the whole image e.g. based on the shape of the intensity histogram (Sezan, 1990), applying a Gaussian

Darkner S., B. Dahl A., Larsen R., Skimminge A., Garde E. and Waldemar G. (2010).
LOCAL SEGMENTATION BY LARGE SCALE HYPOTHESIS TESTING - Segmentation as Outlier Detection.
In *Proceedings of the International Conference on Computer Vision Theory and Applications*, pages 215-220
DOI: 10.5220/0002845402150220

mixture model (Hastie et al., 2001) or by performing clustering (Otsu, 1975). Local methods have an adaptive threshold, which varies across the image. As a result the local methods are suited for images with global intensity variations (Stockman and Shapiro, 2001).

Images with regions of interest taking up a small proportion of the image poses a challenge. Histogram shape or clustering methods will be inadequate for finding a good threshold since the regions of interest will almost invisible in the histogram. (Ng, 2006) suggested a threshold at a valley in the histogram while maximizing the between segment variation similar to Outss method (Otsu, 1975). This requires a two-peaked distribution of the histogram, which limits the applicability of the method.

Our method provides a good solution to a wider class of intensity distribution. It can be applied both as a global and local segmentation method which makes it very flexible. Our approach is based on the assumption of a given intensity distribution that can be estimated from the observed distribution. For each intensity value there is a probability of belonging to this distribution, which can be compared to the actual observed distribution. The difference between the expected distribution and the observed can be interpreted as false discoveries used for identifying the threshold value. This idea originates from (Efron, 2004), who used it for identifying observations of interest in genome responses.(Darkner et al., 2007) Applied it for shape analysis.

The rest of the paper is organized as follows. First we describe the details of our method, and following that we describe and discuss our experiments, and finally we conclude our work.

3 LARGE SCALE HYPOTHESIS TESTING

The point of large-scale testing is to identify a small percentage of interesting cases that deserve further investigation using parametric modeling. The problem is that a part of the interesting observations may be extracted, but if more are wanted then also unacceptably many false discoveries are identified (Efron, 2004). A major point of employing large-scale estimation methods is that they facilitate the estimation of the empirical null density rather than using the theoretical density. The empirical null may be considerably more dispersed than the usual theoretical null distribution. Besides from the selection of the non-null cases (the selection problem) large-scale testing also provides information of measuring the effectiveness of the test procedure (estimation problem). In this paper we employ both measures to separate the particles from the background transform calibration images into binary images, segment the corpus callosum and separate white and gray matter in brain images. Simultaneous hypothesis testing is founded on a set of N null hypotheses $\{H_i\}_{i=1}^N$, test statistics which are possibly not independent. $\{Y_i\}_{i=1}^N$ and their associated p-values $\{P_i\}_{i=1}^N$ defining how strongly the observed value of Y_i contradicts H_i.

3.1 False Discovery Rate

In this paper we assume the N cases are divided into two classes, Null and non-null occurring with prior probabilities p_0 and $p_1 = 1 - p_0$. We denote the density of the test statistics given its class $f_0(z)$ and $f_1(z)$ (null or non-null respectively). False discovery rate (FDR) methods are central to some large scale method and is employed here. It is typical to consider the actual distribution as a mixture of outcomes under the null and alternative hypotheses. Assumptions about the alternative hypothesis may be required. The subdensities

$$f_0^+(z) = p_0 f_0(z) \quad , f_1^+(z) = p_1 f_1(z) \tag{1}$$

and mixture density

$$f(z) = f_0^+(z) + f_1^+(z) \tag{2}$$

leads directly to the local false discovery rate:

$$\begin{aligned} fdr(z) &\equiv P(null|z_i = z) \\ &= p_0 f_0(z)/f(z) = f_0^+(z)/f(z) \end{aligned} \tag{3}$$

The FDR describes the expected proportion of false positive results among all rejected null hypotheses and guarantees that the fraction of the number of false positives over the number of tests in which the null hypothesis was rejected (Efron, 2004). Figure 1 and 2 illustrates the fundamentals of the approach.

For segmentation of particles the hypothesis test is used to find pixels that are a part of a segment i.e. observations that deviates significantly from the average local background. We use large-scale testing to estimate the empirical null hypothesis for a given region assuming the pixel values follows some normal distribution. It is convenient to consider $z_i = \Phi^{-1}(P_i), \quad i = \{1 \ldots N\}$ where Φ is the standard normal cdf and $z_i|h_i \sim N(0,1)$. Estimates of the pixel error and confidence bounds can be mapped to $N(0,1)$ through Φ. As an example of prior information for particles we see that the background has higher pixel intensities than the particles. The background will therefor be the highest and largest distribution. This can be used to get a better empirical estimate of of the null hypothesis.

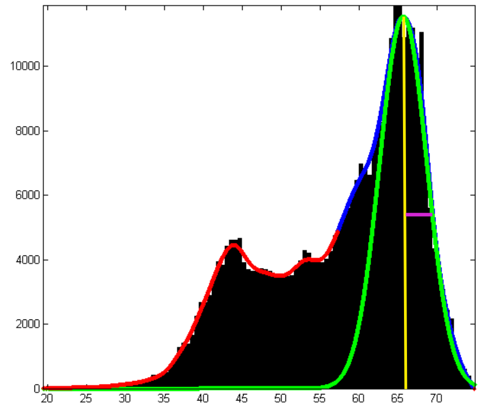

Figure 1: The graphical presentation of large scale hypothesis test. The red and blue curve is $f(z)$, the green is the pdf of the estimated null hypothesis $f_0^+(z)$ where the yellow is the mean and the purple is the half width half maximum.

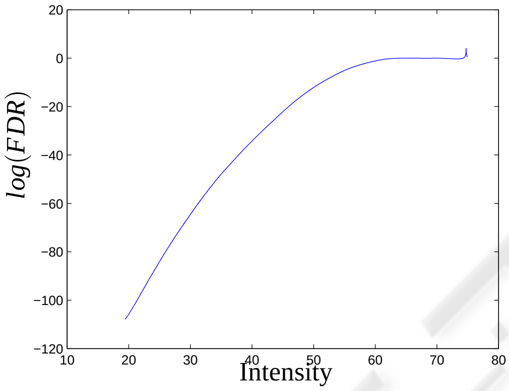

Figure 2: The corresponding logarithm of FDR for Figure 1.

3.2 Estimation of H_0

Assuming that the prominent distribution follows a normal distribution we are able to estimate H_0. Thus for the estimation we choose an appropriate resolution and map all value into the histogram. This forms our joint distribution $f(z)$ to which we then fit a spline with appropriate smoothness for an approximation of the joint distribution. We can then identify the first large peak as the mean value of $f_0^+(z)$ and use half width, half maximum to estimate the standard deviation i.e. the maximum peak of $f(z)$ and half of the width (see Figure 1). The obvious choice would be full width half maximum, however there is a blending of in the joint distribution of $f_0^+(z)$ and $f_1^+(z)$ which gives a thicker tail towards lower intensity values and a much more conservative estimate of the standard deviation (see Figure 1). The estimation of $f_0^+(z)$ is a good place to apply prior knowledge of the distributions such as ordering etc.

3.3 Parameters and Their Interpretation

In practice several parameter have to be selected. The first is the level at which we are willing to accept false positives which is the an expression of the certainty that a given observation is significantly different from H_0. This does not in anyway tell us that the class is a certain kind of tissue or particle, only that this is with certainty p different from the null distribution thus the observation is an outlier.
The testing area has to be selected. This criteria is mainly driven by the object in question and the background. Sufficient information about the distribution of the object and background must be present. The spatial sampling density has to be selected as well. In all experiments in this paper we have up-sampled the image by a factor of 10-100 which also yields an equal sub-pixel resolution of the method. Usually the test is based on $10^5 - 10^6$ samples and in a 100 bin histogram which ensures smooth estimate of $f(z)$ and enough resolution for gray values. In practice $f(z)$ is approximated by a spline thus the smoothness has to be selected for good estimation of $f_0^+(z)$ and can compensate for low number of sample.

4 EXPERIMENTS

We have applied the method to 3 sets of data. Small particles obtained with high magnification, 2D slices of brain MRI for segmentation of the Corpus Callosum and a standard checker board for image calibration with highly varying intensity values. These 3 diverse applications show the versatility of this simple but robust method. For all examples we have shown the sampling area in the sampling resolution for both segmentation and object.

4.1 Particles

For characterization of powders, droplets etc the size and shape of the objects are very important. In order to do a good classification the particles need to be found and properly segmented. The method is well suited for images where the light source changes in intensity and distribution locally (e.g. shadows) and globally (e.g. illumination) from frame to frame in a series of images, cases where robust estimate for background removal can be difficult to obtain. In addition some particles may partially shadow other particles thus making the global background removal incapable of segmenting the particle in question. The method has been tested on 3 types of particle images.

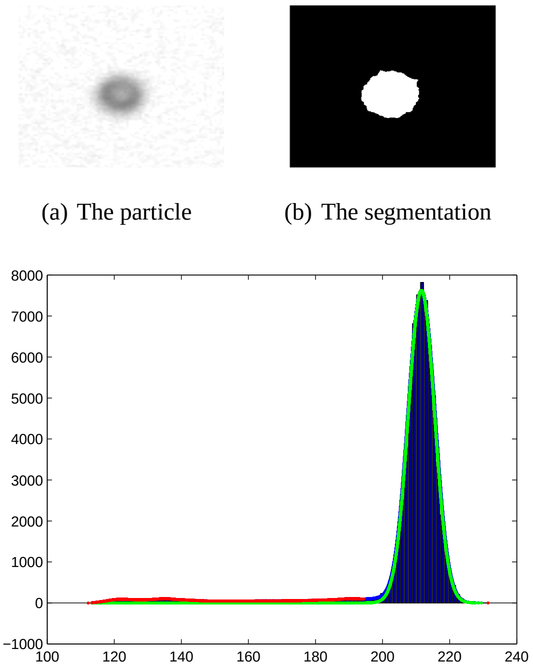

(a) The particle

(b) The segmentation

(c) The hypothesis test histogram

Figure 3: A typical segmentation and the corresponding histogram. The green line in the histogram is the estimated H_0 and the red line indicates outlier with the fdr=0.0001 The histogram clearly show how well our assumption of the background following a normal distribution holds. The outlier are the particle we segmenting.

A set of LED back lit particles suspended between 2 sheets of glass with varying distance to the focus plane . A tracking scenario with time series of calibrated particles suspended in water and laser back lit non-uniform particles suspended in water.

4.1.1 Fixed Particle

We have applied the method to the 25 μ m particles suspended in water between two sheets of glass in with different distances to the focal plane. Figure 4 show a 25 μ m particle at 6 distances to the focal plane. This experiment illustrates the sensitivity of the method, where even vaguely visible particles can be segmented without parameter tuning. The threshold was selected on the criteria that the possibility of a false positive should be less than 0.01%, the size of the window is 40 × 40 and the sampling resolution in each direction is 0.1 pixel.

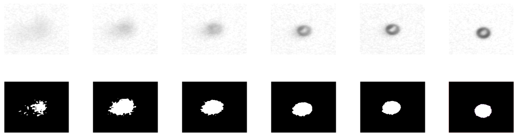

Figure 4: The images show the particle at 6 different distances to the focal plane, with the las image being of the particle in focus. Below are the segmentations of each od the images in the same order. The images show that the particle can be segmented even if the signal is very vague and the glare point is correctly classified as a part of the particle.

4.1.2 Shadowing Effect

We have preprocessed all images with multi scale blob detection (Bretzner and Lindeberg, 1998) such that we have rough estimate of the size and location of the blobs. This is sufficient to perform the segmentation. The data consists of movie sequences obtained with 5 times magnification of semi transparent particles of 100, 50, 25 and 5 μm in a water solution and used for illustration of handling of shadowing effects without change to the parameters of the algorithm. Figure 5 show a segmentation performed over several frames where a larger particle passes in the background creating a shadowing effect. The example illustrates how the methods can handle changes in the illumination without failure. The threshold was selected with $p = 0.0001$, windowsize of 20×20 pixel with a sampling resolution of 0.1 pixel.

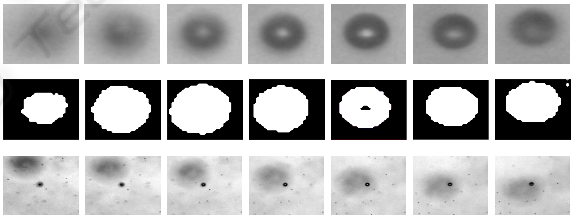

Figure 5: The figure show a segmentation performed with the same parameters on the same object subject to changing shadowing effect caused by a large particle passing in the background.

4.1.3 Real Particles

To show how the method handles real world data we have segmented some particles of some material samples from the industry. Figure 6 and 7 show two small examples of such particles. The segmentation is very good due to the locally very uniform background, making the distribution of peaked and narrow i.e. a small standard deviation. Glare points are also handled very well but there is naturally enough a band around the glare point where the particle is misclassified. This is due to the fact that the method is just a simple threshold without any spatial prior. These gaps can be handled by applying an appropriate post processing step. The results in figure 6 was made with $p = 0.0001$ and a window of 200×200 with a sampling resolution of 0.3 pixels and the results in figure 7 with a window of 100×100 same p and same resolution.

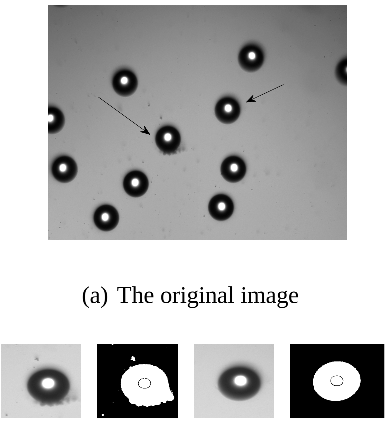

(a) The original image

Figure 6: The figure show some real world samples. The figure show that the segmentation the glare points is handled very well. The small 'gap' can be fixed by a simple morphological operation.

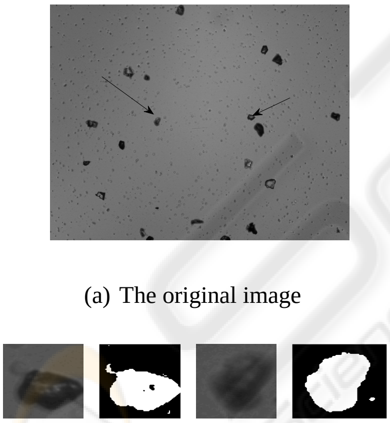

(a) The original image

Figure 7: Some crystal like particles are shown in the figure. In spite of the relative low difference between background and object and the fact that the samples are semi transparant, the segmentation is good. Even small ones are handled together with the large ones.

4.2 Calibration Images

We also present some results on calibration images. When using a well known structure as the checkerboard for calibration it is important to exactly locate the corner of the squares i.e. by morphological operations on a segmented image. The proposed method delivers very good segmentation and it is expected that it can be used to derive the exact sub-pixel position of the corners creating a robust foundation for image calibration. Figure 8 and 9 show the results of the segmentation. The results in Figure 9 was made with $p = 0.0001$ and a window of 100×100 with a sampling resolution of 0.3 pixels.

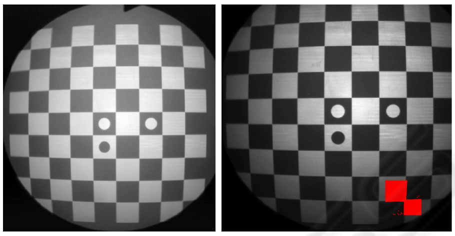

(a) The calibration image

(b) The calibration image with the segmentation marked

Figure 8: The original calibration image. As can be seen the intensities varies significantly with the highest values at the center and decaying radially.

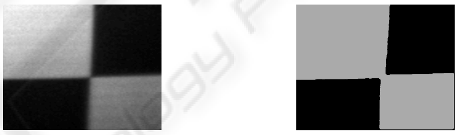

(a) Segmented image part

(b) Segmentation

Figure 9: The changes in gray scale values are handled quite nicely, but causes the little gap between the two black corners in the segmentation. This can be close with morphological operations.

4.3 MRI

To illustrate the method on another modality, we have applied the method to MRI scans of the human human brain, more precisely the midsagittal plane that contain the corpus corpus callosum (see Figure 10(a)). The method has applied to white and gray matter segmentation and segmentation of the corpus callosum. In the latter case we have a manually segmented ground truth, thus we can compute the segmentation error via the Dice coefficient (Sørensen, 1948). The results in Figure 10 was made with $p = 0.01$ and a window of 60×80 with a sampling resolution of 0.1 pixels.

Across 40 subject with their Corpus Callosum segmented with the AAM (Ryberg et al., 2006) and manually corrected we found that local segmentation through large scale hypothesis testing gave an average Dice coefficient of 0.856 with a standard deviation of 0.034. The Corpus Callosum was extracted in the same hypothesis test, however if we use the local

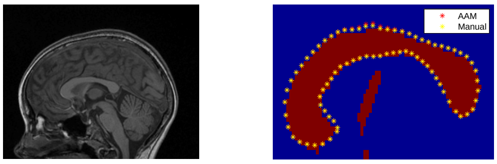

(a) MRI (b) segmentation

Figure 10: (a)The midsagittal slice from an MRI of a head. (b) This figure show the result of the segmentation of fig 10(a) using the method proposed in this paper. The red dots are the segmentation achieved by the AAM and the yellow the manual segmentation. The read part of the image is the segmentation with the our method. This result show how efficient this algorithm is for local segmentation.

property and us a smaller window, outliers become more significant and we get better segmentation. By switching to a more local neighborhood we get a improvement of almost 3% to 0.880 and the difference is very significant $(p << 0.01)$ using a paired t-test. As a last test we separated the white and gray matter. The results are a little greedy, some gray matter is classified as white matter. This is due to the fact that the two density functions are somewhat overlapping and that the dark regions actually is a 3 class segmentation problem making it non-binary. Some improvement can be obtained by adjusting the window size and the p-value. The results in figure 11 were made with $p = 0.01$ and a window of 40×40 with a sampling resolution of 0.1 pixels.

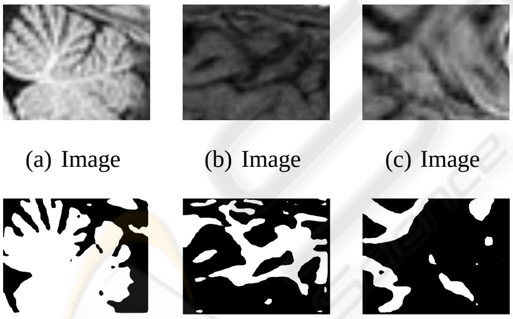

(a) Image (b) Image (c) Image

(d) segmentation (e) segmentation (f) segmentation

Figure 11: Some results on segmenting the white matter. The results are a little greedy including some gray matter.

5 SUMMARY AND CONCLUSIONS

We have presented a local adaptive method for binary segmentation. The methods has successfully been tested on particle images for particle segmentation, calibration images and and midsagittal slices of MRI for segmentation of corpus callosum and gray matter white matter segmentation. The method is very robust with respect to changes in intensity across the image and statistically characterizes the resulting segmentation. We have shown that compared to manual segmentation of the Corpus Callosum we can achieve a dice coefficient of 0.88 on using a mosaic of 5 patches. The method is directly extendable to 3D, other types of distribution. The hypothesis test and FDR should be extended to higher dimensions that the one dimensional case discussed here and tested on several other types of images. furthermore the algorithm should be implemented such that it can handle multiple classes and segment a whole image at once.

REFERENCES

Bretzner, L. and Lindeberg, T. (1998). Feature tracking with automatic selection of spatial scales. *Computer Vision and Image Understanding*, 71(3):385–392.

Darkner, S., Paulsen, R. R., and Larsen, R. (2007). Analysis of deformation of the human ear and canal caused by mandibular movement. In *Medical Image Computing and Computer Assisted Intervention MICCAI 2007*, pages 801–8, B. Brisbane, Australia, Springer Lecture Notes.

Efron, B. (2004). Large-scale simultaneous hypothesis testing: the choice of a null hypothesis. *Journal of the American Statistical Association*, 99(465):96–104.

Hastie, T., Tibshirani, R., and Friedman, J. (2001). *The Elements of Statistical Learning: Data Mining, Inference, and Prediction*. Springer-Verlag.

Ng, H. (2006). Automatic thresholding for defect detection. *Pattern Recognition Letters*, 27(14):1644–1649.

Otsu, N. (1975). A threshold selection method from gray-level histograms. *Automatica*, 11:285–296.

Ryberg, C., Stegmann, M. B., Sjöstrand, K., Rostrup, E., Barkhof, F., Fazekas, F., and Waldemar, G. (2006). Corpus callosum partitioning schemes and their effect on callosal morphometry.

Sezan, M. (1990). A peak detection algorithm and its application to histogram-based image data reduction. *Computer Vision, Graphics, and Image Processing*, 49(1):51.

Sezgin, M. and Sankur, B. (2004). Survey over image thresholding techniques and quantitative performance evaluation. *Journal of Electronic Imaging*, 13(1):146–168.

Sørensen, T. (1948). A method of establishing groups of equal amplitude in plant sociology based on similarity of species content and its application to analyses of the vegetation on Danish commons. *Biologiske Skrifter*, (5):1–34.

Stockman, G. and Shapiro, L. (2001). *Computer Vision*. Prentice Hall PTR, Upper Saddle River, NJ, USA.